Notes

Thin-Film Morphologies and Solution-Processable Field-Effect Transistor Behavior of a Fluorene−Thieno[3,2-*b*]thiophene-Based Conjugated Copolymer

Eunhee Lim,[†] Byung-Jun Jung,[†,§] Jaemin Lee,[†,⊥] Hong-Ku Shim,[*,†] Jeong-Ik Lee,[‡] Yong Suk Yang,[‡] and Lee-Mi Do[‡]

Department of Chemistry and School of Molecular Science (BK21), Center for Advanced Functional Polymers, Korea Advanced Institute of Science and Technology, Daejeon 305-701, Korea, and Electronics and Telecommunications Research Institute, Daejeon 305-350, Korea

Received September 13, 2004
Revised Manuscript Received March 20, 2005

Introduction

Interest in organic semiconductors has increased in recent years due to their potential applications in optoelectronic devices such as light-emitting diodes (OLEDs),[1−3] thin-film transistors (TFTs),[4−8] and photovoltaic devices.[9,10] Organic electronic devices such as these have various advantages over conventional inorganic electronics, including facile processability, chemical tunability, compatibility with plastic substrates, and low-cost processing. Among the potential applications of organic semiconductors, organic TFTs can be used in low-cost memories, smart cards, and the driving circuits of large-area display devices.[11−13] To date, the highest field effect mobility values for organic TFTs have been achieved with vapor-deposited purified pentacene films.[14] However, to minimize manufacturing costs, the TFT fabrication process should ideally include solution-based methods such as spin-coating, stamping, or ink-jet printing. In recent years, most solution-processable conjugated materials have been based on polythiophenes due to their good electrical conductivity as p-type semiconductors. Improvements in fabrication techniques have enhanced the performance of solution-processed polymer TFTs to a point where they are now approaching inorganic amorphous silicon TFTs, with mobilities of 0.05−0.1 $cm^2\ V^{-1}\ s^{-1}$ and on/off current ratios of $>10^6$.[15] In addition, the use of soluble polymeric semiconductors has made possible the development of active-matrix multipixel displays using solution-based technologies.[16]

More recently, fluorene-based block copolymers have attracted much attention as promising materials for polymer TFTs. Interest in these copolymers was sparked by work showing that enhanced charge carrier mobilities were achieved in poly(9,9′-*n*-dioctylfluorene-*alt*-bithiophene) (F8T2) by aligning the polymer chains in the liquid-crystalline (LC) phase.[17,18] In addition, F8T2 was shown to be more resistant against chemical doping by atmospheric oxygen than other polymeric semiconductors such as poly(3-hexylthiophene).

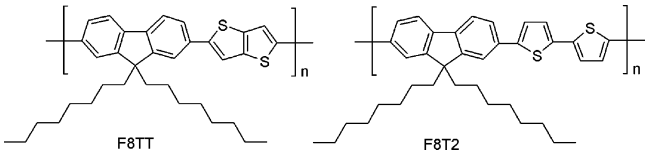

Figure 1. Chemical structures of F8TT and F8T2.

To obtain high carrier mobilities, it is crucial that the organic molecules be arranged in specific molecular architectures. For example, the introduction of fused ring compounds such as pentacene, bis(dithienothiophene), benzodithiophene, and anthradithiophenes into organic TFTs has been shown to result in improved TFT performance due to enhanced intermolecular ordering and $\pi-\pi$ stacking.[14,19,20] We hypothesized that, even in a polymeric system, a higher degree of order can be obtained by introduction of groups with high degrees of planarity and rigidity. Therefore, in the present work we introduced a fused ring compound, the thieno[3,2-*b*]thiophene group, into a fluorene-based alternating copolymer. We found that more crystalline polymers gave better TFT device performance. The present results provide valuable information on the relationship between the molecular structure of a semiconducting material and its electrical performance in thin film electronic devices.

Experimental Section

Materials. Poly(9,9′-*n*-dioctylfluorene-*alt*-thieno[3,2-*b*]thiophene) (F8TT), poly(9,9′-*n*-dioctylfluorene-*alt*-bithiophene) (F8T2), and poly(9,9′-*n*-dioctylfluorene) (F8) were synthesized according to the literature method.[21] The chemical structures of the polymers are shown in Figure 1. The number-average molecular weights (M_n) of the polymers, F8TT, F8T2, and F8 are 23 000 ($M_w/M_n = 2.8$), 31 000 ($M_w/M_n = 2.4$), and 35 600 ($M_w/M_n = 2.8$), respectively.

XRD Measurements. Films of F8TT and F8T2 of thickness ca. 5 μm were prepared on quartz glass substrates by solution-casting of the polymers dissolved in dichlorobenzene (>3 wt %). These films were annealed at above the liquid-crystalline melting temperature (annealing temperatures of 285 °C) and then cooled to room temperature. A film of a well-known liquid-crystalline polyfluorene homopolymer, F8, was also prepared in the same way (annealing at 160 °C) for comparison. X-ray diffraction patterns were recorded in the reflection mode at 30 kV and 60 mA with a scanning rate of 0.03° per 60 s and Cu Kα radiation (with wavelength $\lambda = 1.5406$ nm).

Fabrication of Organic TFT Devices. Thin-film transistors were fabricated using the bottom contact geometry (channel length $L = 10\ \mu$m, width $W = 100\ \mu$m). This geometry was chosen over the top contact geometry, which has a higher

[†] Korea Advanced Institute of Science and Technology.
[‡] Electronics and Telecommunications Research Institute.
[§] Current address: Corporate R&D Center, Samsung SDI Co. Ltd., Yongin-Si, Gyeonggi-Do 449−577, Korea.
[⊥] Current address: Corporate R&D Center, LG Chem Research Park, Daejeon 305−380, Korea.
* To whom correspondence should be addressed. E-mail: hkshim@kaist.ac.kr.

10.1021/ma048128e CCC: $30.25
Published on Web 04/15/2005

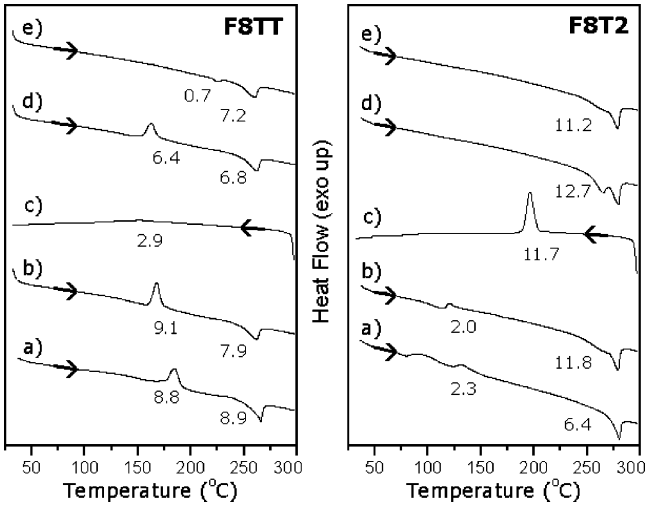

Figure 2. DSC thermograms of F8TT (left, sample weight: 4.9 mg) and F8T2 (right, sample weight: 5.2 mg) for the following thermal cycles: (a) heating at 10 °C/min of pristine sample; (b) heating at 10 °C/min after quenching from 300 °C; (c) slowly cooling at 10 °C/min after equilibration at 300 °C; (d) heating at 10 °C/min after slowly cooling from 300 °C; (e) heating at 10 °C /min after quenching from 220 °C. The enthalpic changes (J/g) are shown at each transition.

mobility, on account of the practical consideration that organic TFTs will ultimately be manufactured in the bottom contact configuration.[22] In our devices, source and drain contacts consisted of gold and the dielectric was silicon oxide (SiO_2) with a thickness of 300 nm. The SiO_2 surface was cleaned, dried, and pretreated with hexamethyldisilazane (HMDS)[15] to produce apolar and smooth surfaces onto which the polymer could be spin-coated. The polymers were dissolved in 0.5 wt % dichlorobenzene and filtered through a 0.45 μm pore size poly(tetrafluoroethylene) (PTFE) membrane syringe filter before use. The polymer solutions were heated to 80 °C to make them compatible with the spin-coating process and then applied dropwise onto the substrates and spin-coated at 1500 rpm. The polymeric devices exhibited good stability to atmospheric oxygen and could be handled without the use of a glovebox.

Results and Discussion

Liquid Crystalline Properties. Before examining thin film morphologies and FET characteristics of semiconducting materials, it is important to clearly identify the phase transition behaviors. Particularly in liquid-crystalline polymers, the transition temperatures must be attained in order for annealing processes to align polymer chains.[17] Figure 2 shows differential scanning calorimetry (DSC) scans of the polymers (left: F8TT; right: F8T2). Both polymers showed typical LC characteristics, i.e., both exothermal crystalline and endothermal melting peaks. The crystallization and melting peaks of F8TT appear in the ranges 160−185 and 260−265 °C, respectively (line a), and recrystallization occurs at around 151 °C on slow cooling (line c). The crystallization and melting peaks of F8T2 appear in the ranges 120−132 and 263−280 °C, respectively (line a), and recrystallization occurs at 195 °C on slow cooling (line c). The transition temperatures and the shape of transitions vary with pretreatment methods. The transition temperatures of the polymers were relatively higher than those used in our previous study[21] due to the higher molecular weight.

In F8TT, the phase transitions of crystalline and liquid-crystalline states appeared at both heating scans of line b and d. However, the enthalpic changes of crystallization were distinctly different: the degree of

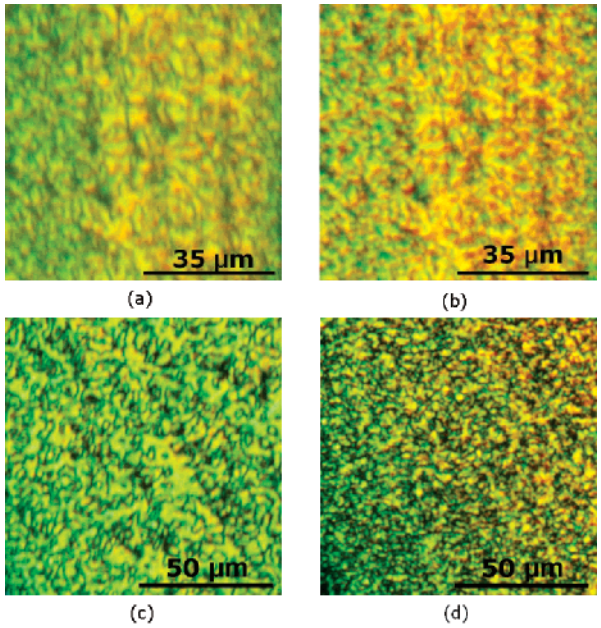

Figure 3. Optical micrographs through crossed polarizers of an F8TT film (magnified 200×). (a) The film was heated to 285 °C and (b) quenched to room temperature. (c) The film was heated to 285 °C and (d) cooled to room temperature at 10 °C/min.

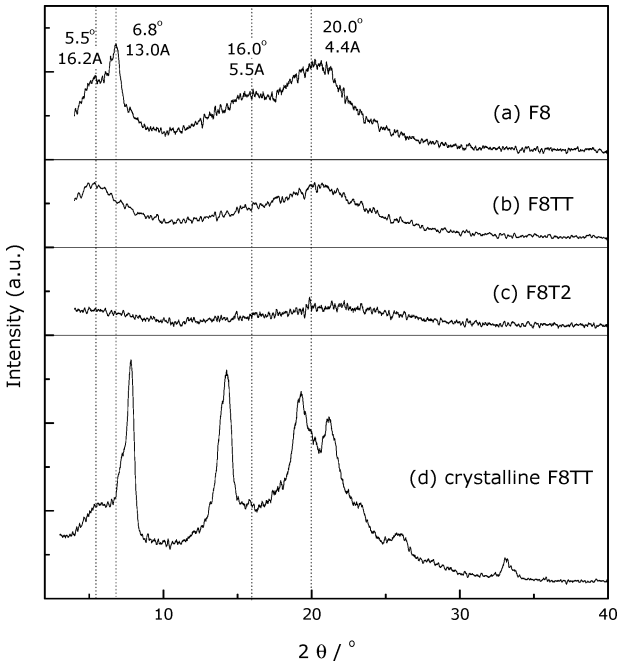

Figure 4. XRD patterns of the nematic quenched liquid-crystalline (a) F8, (b) F8TT, and (c) F8T2 films and crystalline (d) F8TT film.

crystallization of the quenched sample (line b) is larger by ~2.5 J/g than that of the sample cooled slowly (line d). This difference corresponds with the enthalpic change (~2.9 J/g) of a broad exothermal recrystallization peak in F8TT in the slow cooling scan (line c). This indicates that the recrystallization of F8TT during the cooling process can be almost completely suppressed by quenching. On the other hand, F8T2 showed a clearly defined recrystallization peak at 195 °C in the slowly cooling scan (line c) and no exothermal phase transition in the heating scan after slowly cooling from 300 °C (line d). This indicates that F8T2 completely recrystallizes while it is cooled slowly at a rate of 10 °C/min. The

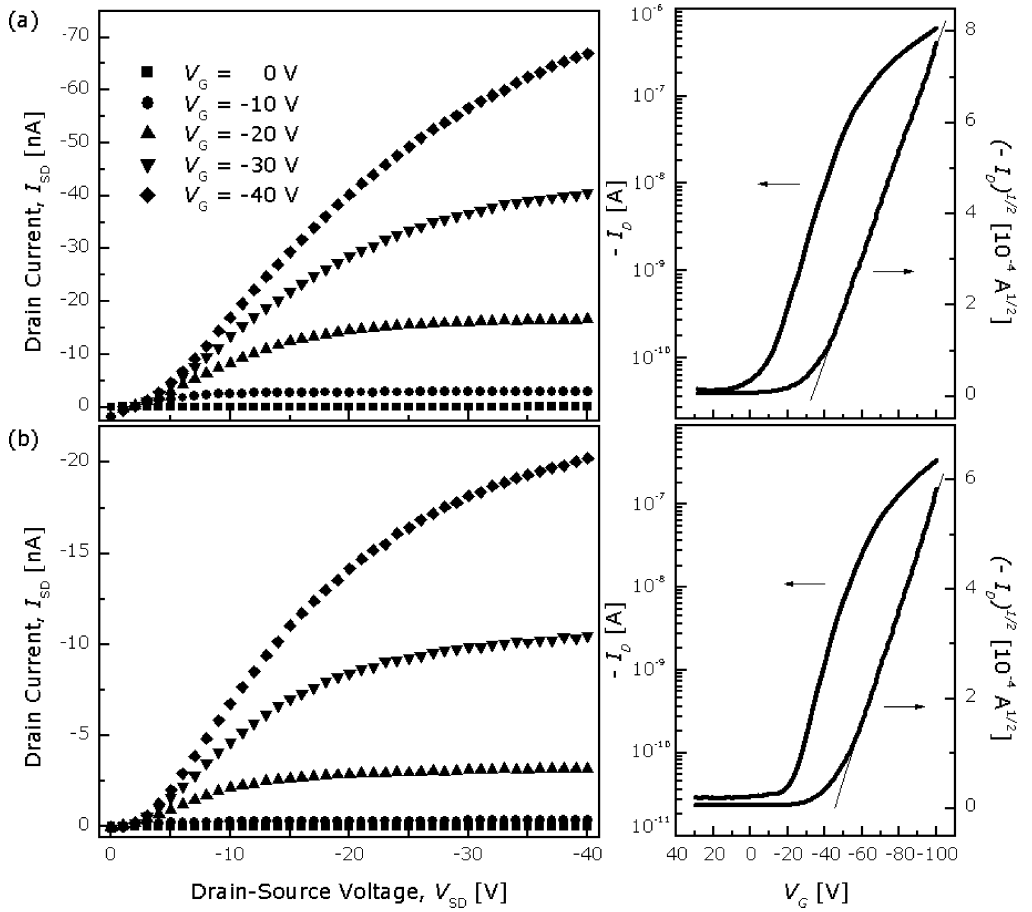

Figure 5. Output characteristics of the TFT devices at different gate biases (left) and plots of the transfer at constant $V_D = -100$ V (right) (semilogarithmic plot of $-I_D$ vs V_G (left axis) and plot of $(-I_D)^{1/2}$ vs V_G (right axis)) for devices using (a) F8TT and (b) F8T2.

enthalpic changes of F8T2 upon cooling depended on the cooling rates. As the sample was cooled faster, the enthalpic changes of F8T2 upon cooling were smaller. Further, the quenched F8T2 crystallized upon heating at 120 °C with enthalpic change of ~2 J/g (line b). This means that recrystallization of F8T2 during cooling can be partially suppressed by quenching. It has been reported that if recrystallization occurs on cooling the mobility of the resulting polycrystalline films can be lowered due to carrier trapping at grain boundaries.[23] Therefore, it is important to generate a liquid-crystalline glassy morphology of the polymer films so as not to lose high mobility. From this DSC study, we have confirmed that the recrystallization of F8TT on cooling is clearly suppressed. It is concluded that F8TT films in a liquid-crystalline melt state can be achieved by quenching after equilibration above their melting transition.

In addition, the polymers were preheated to 220 °C (above their exothermal crystalline peaks) and rapidly quenched to room temperature (line e). Exothermal crystallization peaks upon reheating were not observed in either polymer, indicating that quenching after equilibration at 220 °C will yield polymers in a crystalline state.

Polarized optical microscopy (PLM) of the polymer films was also used to determine the thermal liquid crystalline properties of the polymers (Figure 3). Figure 3a shows a transmission polarized optical micrograph of an F8TT film heated to 285 °C. Above their melting temperatures, the films of the polymers showed characteristic nematic liquid-crystalline texture. Subsequently, after quenching to room temperature, the F8TT film still displayed a birefringent fluid phase (Figure 3b). For comparison, the film heated to 285 °C (Figure 3c) was cooled slowly at a rate of 10 °C/min to room temperature. Compared with the quenched film, a slowly cooled film showed some crystallization changes, as shown in Figure 3d. From this, we can assume that partial recrystallization occurred on slow cooling is suppressed by quenching, which is consistent with the phase transition characteristics revealed by DSC analysis.

XRD Analysis. Crystallization of the polymers was confirmed by film X-ray diffraction (XRD) studies, which allowed identification of the nature of the mesophase. XRD patterns of the polymers are shown in Figure 4. The nematic films of F8 (a) and F8TT (b) showed a peak at ca. 5.5°; however, no corresponding diffraction peak was observed for F8T2 (c). These peaks are consistent with the previously reported layer periodicities observed for alkyl-substituted fluorene- or thiophene-based polymers.[24−27] The peak at ca. 5.5° corresponds to a layering distance, d_{100} = 16.2 Å, between sheets of polymer chains which pack in a plane perpendicular to their longitudinal axes. In contrast to the oligomeric molecules,[28] in polymeric semiconducting materials the polymer backbones lie parallel to the substrate surface, and there is interdigitation of the side chains of neighboring polymer backbones. Therefore, the layers of polymer backbones are separated from each other by the alkyl side chains, which are oriented normal to the aromatic planes. The alignment of polymer chains is

important to the carrier transfer in polymer FETs. This enhanced alignment of the polymer backbone of F8TT is likely due to the rigidity of the thieno[3,2-*b*]thiophene group. In addition to that, for all polymers, the scans of intensity vs 2θ (0°−50°) show broad diffraction peaks at ca. 20°, which correspond to a d spacing of ca. 4.4 Å. These peaks have been attributed to the lateral distance between polymer chains within the layer planes or side-chain crystallization.[29]

Compared to the XRD patterns of the nematic F8TT film (Figure 4b), the sharp peaks at 7.9° and 14.3° appeared distinctively in the slowly cooled F8TT film (Figure 4d). It is already reported that XRD of thin polyfluorene films show different diffraction patterns in the crystalline and LC states.[25] In their work, the film in the LC phase loses macroscopic ordering in the plane of the surface which exists in the crystalline phase. Recently, Su et al. reported on the characteristic XRD profiles for F8 films composed of N (quenched from LC to 0 °C) and crystalline (α, α', and β) phases.[30,31] In their work, the nematic liquid crystalline film (prepared by quenching from above the melting temperature) showed weak and broad halos centered at $2\theta = 5.5°$ and 20°. The difference of crystalline and LC phases of polyfluorene homopolymer (F8) was also observed in our work with F8TT. The quenched nematic liquid-crystalline F8TT film showed different XRD patterns from that of the crystalline phase F8TT film.

FET Characteristics. The thin-film transistors of F8TT and F8T2 showed typical p-channel FET characteristics (Figure 5); i.e., when a negative bias was applied, the drain-source current scaled with the negative gate voltage due to the increased number of charge carriers (holes). Plots of the transfer curve [i.e., $I_D = f(V_G)$] at constant $V_D = -100$ V are shown in Figure 5. The field-effect mobilities were calculated in the saturation regime[22] at a drain voltage of $V_D = -40$ V and the on/off ratios at a drain voltage of $V_D = -100$ V.

The films were annealed at 285 °C for 10 min and quenched to room temperature to maintain the liquid-crystalline alignment of the polymer chains. A thin film of F8TT gave an FET mobility of 1.1×10^{-3} cm^2 V^{-1} s^{-1} and an on/off ratio of 1.4×10^4 without the use of any alignment technique; this mobility was 3 times higher than the mobility of F8T2 (0.4×10^{-3} cm^2 V^{-1} s^{-1}) under the same conditions. The higher performance of F8TT indicates that this polymer has a well-defined molecular architecture, consistent with the morphologic characteristics revealed by XRD analysis. The change of a relatively flexible bithiophene to a rigid fused thieno[3,2-*b*]thiophene results in higher crystallinity and a more ordered morphology. This trend is consistent with previous studies on linear compounds, which indicate that mobility tends to increase with increasing molecular rigidity.

In addition, the F8TT film that slowly cooled to room temperature after being annealed at 285 °C showed relatively low FET mobility of an order of 10^{-5} cm^2 V^{-1} s^{-1}. It is caused by the partial recrystallization of the film of F8TT on slowly cooling, as characterized above with DSC and PLM studies. The recrystallization that occurred during the cooling process can lower the mobility of the resulting polycrystalline films through carrier trapping at grain boundaries.[23] In other words, to the use of fluorene- and thiophene-based liquid-crystalline polymers as semiconducting layers, a liquid-crystalline glassy morphology of the polymer films has to be maintained on cooling to get a high charge carrier mobility. In this study, F8TT films in a liquid-crystalline melt state can be achieved by quenching after equilibration above their melting transition.

The fluorene-based block copolymers prepared in the present work showed significantly low off-currents (e.g., 42 pA for F8TT), which can be attributed to the stable (more negative) HOMO energy levels in these polymers (e.g., −5.38 eV for F8TT[21]). Similar correlations between off-current and HOMO (or LUMO) energy have been reported for thiophene−phenylene and thiophene−thiazole semiconductors (or n-channel semiconductors).[32]

The electrical properties of devices based on F8T2 are strongly dependent on the device structure and the fabrication method. We believe that organic TFTs could be further improved by optimizing the fabrication conditions such as the suitable choice of gate insulator materials and the surface treatment by chemical modification of the SiO_2 surface.[33−35] In addition, it may also be possible to align these polymers from their LC phase with the help of an alignment layer so as to achieve desirable molecular orientations, which would improve the performance of thin film electronic devices based on these polymers.

Conclusion

We have successfully synthesized a fluorene- and thieno[3,2-*b*]thiophene-based copolymer suitable for use as semiconducting materials in solution-processable organic field-effect transistors. Replacement of the relatively flexible bithiophene in F8T2 with a rigid fused thieno[3,2-*b*]thiophene yielded a polymer (F8TT) with higher crystallinity and a more ordered morphology. Because of this enhanced molecular ordering, F8TT FET devices exhibited improved mobilities of up to 1.1×10^{-3} cm^2 V^{-1} s^{-1}, which is 3 times higher than the mobility of F8T2 devices. Further improvements in the performances of TFTs based on F8TT should be possible by the optimization of the fabrication conditions and/or the alignment technique for molecular orientation. The present findings on the relationship between the crystallinity of semiconducting materials and their electrical properties provide useful guidelines for the molecular design of high mobility conjugated polymers for OTFT applications.

Acknowledgment. This work was supported by the Information Display R&D Center (No. AOD 02-A) through 21st Century Frontier R&D Program of Ministry of Science and Technology (MOST). We gratefully acknowledge Dr. T. Hayakawa, Dr. Tokita, Mr. M. Seo, Mr. Sato, and Prof. T. Yamamoto for the helpful discussion on XRD studies.

Supporting Information Available: Measurements, additional figures including DSC thermograms and device configuration, and the summarized device characteristics. This material is available free of charge via the Internet at http://pubs.acs.org.

References and Notes

(1) Burroughes, J. H.; Bradley, D. D. C.; Brown, A. R.; Marks, R. N.; Mackey, K.; Friend, R. H.; Burns, P. L.; Holmes, A. B. *Nature (London)* **1990**, *347*, 539.

(2) Friend, R. H.; Gymer, R. W.; Holmes, A. B.; Burroughes, J. H.; Marks, R. N.; Taliani, C.; Bradley, D. D. C.; Dos Santos,

D. A.; Brédas, J. L.; Lögdlund, M.; Salaneck, W. R. *Nature (London)* **1999**, *397*, 121.
(3) Shim, H.-K.; Jin, J.-I. *Adv. Polym. Sci.* **2002**, *158*, 193.
(4) Katz, H. E.; Bao, Z.; Gilat, S. L. *Acc. Chem. Res.* **2001**, *34*, 359.
(5) Horowitz, G. *Adv. Mater.* **1998**, *10*, 365.
(6) Meng, H.; Bao, Z.; Lovinger, A. J.; Wang, B.-C.; Mujsce, A. M. *J. Am. Chem. Soc.* **2001**, *123*, 9214.
(7) Babel, A.; Jenekhe, S. A. *Macromolecules* **2003**, *36*, 7759.
(8) Yamamoto, T.; Kokubo, H.; Kobashi, M.; Sakai, Y. *Chem. Mater. Macromol.* **2004**, *16*, 4616.
(9) Schmidt-Mende, L.; Fechtenkötter, A.; Müllen, K.; Moons, E.; Friend, R. H.; MacKenzie, J. D. *Science* **2001**, *293*, 1119.
(10) Brabec, C. J.; Sariciftci, N. S.; Hummelen, J. C. *Adv. Funct. Mater.* **2001**, *11*, 15.
(11) Crone, B.; Dodabalapur, A.; Lin, Y.-Y.; Filas, R. W.; Bao, Z.; LaDuca, A.; Sarpeshkar, R.; Katz, H. E.; Li, W. *Nature (London)* **2000**, *403*, 521.
(12) Gelinck, G. H.; Geuns, T. C. T.; de Leeuw, D. M. *Appl. Phys. Lett.* **2000**, *77*, 1487.
(13) Klauk, H.; Jackson, N. *Solid State Technol.* **2000**, *43*, 63.
(14) Dimitrakopoulos, C. D.; Purushothaman, S.; Kymissis, J.; Callegari, A.; Shaw, J. M. *Science* **1999**, *283*, 822.
(15) Sirringhaus, H.; Tessler, N.; Friend, R. H. *Science* **1998**, *280*, 1741.
(16) Huitema, H. E. A.; Gelinck, G. H.; van der Putten, J. B. P. H.; Kuijk, K. E.; Hart, C. M.; Cantatore, E.; Herwig, T.; van Breemen, A. J. J. M.; de Leeuw, D. M. *Nature (London)* **2001**, *414*, 599.
(17) Sirringhaus, H.; Wilson, R. J.; Friend, R. H.; Inbasekaran, M.; Wu, W.; Woo, E. P.; Grell, M.; Bradley, D. D. C. *Appl. Phys. Lett.* **2000**, *77*, 406.
(18) Sirringhaus, H.; Kawase, T.; Friend, R. H.; Shimoda, T.; Inbasekaran, M.; Wu, W.; Woo, E. P. *Science* **2000**, *290*, 2123.
(19) Laquindanum, J. G.; Katz, H. E.; Lovinger, A. J. *J. Am. Chem. Soc.* **1998**, *120*, 664.
(20) Laquindanum, J. G.; Katz, H. E.; Lovinger, A. J.; Dodabalapur, A. *Adv. Mater.* **1997**, *9*, 36.
(21) Lim, E.; Jung, B.-J.; Shim, H.-K. *Macromolecules* **2003**, *35*, 4288.
(22) Dimitrakopoulos, C. D.; Malenfant, R. L. *Adv. Mater.* **2002**, *14*, 99.
(23) Redecker, M.; Bradley, D. D. C.; Inbasekaran, M.; Woo, E. P. *Appl. Phys. Lett.* **1999**, *74*, 1400.
(24) Grell, M.; Bradley, D. D. C.; Ungar, G.; Hill, J.; Whitehead, K. S. *Macromolecules* **1999**, *32*, 5810.
(25) Kawana, S.; Durrell, M.; Lu, J.; Macdonald, J. E.; Grell, M.; Bradley, D. D. C.; Jukes, C.; Jones, R. A. L.; Bennett, S. L. *Polymer* **2002**, *43*, 1907.
(26) Yamamoto, T.; Kokubo, H.; Morikita, T. *J. Polym. Sci.*, *Part B*: *Polym. Phys.* **2001**, *39*, 1713.
(27) Bao, Z.; Dodabalapur, A.; Lovinger, A. J. *Appl. Phys. Lett.* **1996**, *69*, 4108.
(28) Garnier, F.; Yassar, A.; Hajlaoui, R.; Horowitz, G.; Deloffre, F.; Servet, B.; Ries, S.; Alnot, P. *J. Am. Chem. Soc.* **1993**, *115*, 8716.
(29) Kinder, L.; Kanicki, J.; Petroff, P. *Synth. Met.* **2003**, *405*, 179.
(30) Chen, S. H.; Su, A. C.; Su, C. H. *Macromolecules* **2005**, *38*, 379.
(31) Chen, S. H.; Chou, H. L.; Su, A. C.; Chen, S. A. *Macromolecules* **2004**, *37*, 6838.
(32) Hong, X. M.; Katz, H. E.; Lovinger, A. J.; Wang, B.-C.; Raghavachari, K. *Chem. Mater.* **2001**, *13*, 4686.
(33) Veres, J.; Ogier, S. D.; Leeming, S. W.; Cupertino, D. C.; Khaffaf, S. M. *Adv. Funct. Mater.* **2003**, *13*, 199.
(34) Salleo, A.; Chabinyc, M. L.; Yang, M. S.; Street, R. A. *Appl. Phys. Lett.* **2002**, *81*, 4383.
(35) Lee, J.; Shim, H.-K.; Lee, J.-I.; Yang, Y. S.; Kim, S. H.; Chu, H. Y.; Do, L.-M. *Mol. Cryst. Liq. Cryst.* **2003**, *405*, 179.

MA048128E